

Threshold Fatigue Crack Growth and Crack Paths in Heat-treated Nodular Cast Iron

R. Konečná¹, G. Nicoletto², S. Fintová¹, L. Bubenko¹

¹ University of Žilina, Faculty of Mechanical Engineering, Department of Materials Engineering, Univerzitná 1, 01026 Žilina, Slovak Republic, radomila.konecna@fstroj.uniza.sk

² University of Parma, Department of Industrial Engineering, Parco Area delle Scienze, 181/A, 43100 Parma, Italy, gianni.nicoletto@unipr.it

ABSTRACT. *Mechanical strength of nodular cast iron (NCI) can be improved by heat treatment. Isothermal Ductile Iron (IDI) competes for application with Austempered Ductile Iron (ADI). Fatigue crack growth experiments performed on comparable grades of IDI and ADI 1050 are initially reported in this paper. In the case of IDI large specimen-to-specimen variation in K_{ath} compared to rather constant K_{ath} of ADI 1050 were observed. To investigate IDI vs. ADI as far as microstructure- ΔK_{th} relation, the fatigue crack paths through the microstructure was examined to identify the active growth micro-mechanisms and compared.*

INTRODUCTION

Nodular cast iron (NCI) is a widely used construction material. Since fatigue strength is a key material selection property for engineering components subjected to dynamic service loads, high strength NCI, such as austempered ductile iron (ADI) is finding increasing use.

The remarkable properties of ADI are attributed to its unique microstructure consisting of high carbon residual austenite and ferrite, i.e. bainitic matrix. Because of the complicated ADI microstructure it is difficult to define the influence of individual microstructural features on its fatigue properties and fatigue crack growth mechanisms. Austempering to high temperatures produces relatively thick ferrite needles in a carbon-rich austenite matrix. When austempering is carried out at low temperatures, the reaction products resemble bainite. If austempering time is very short, the amount of the austenite transformation is less than 100 % [1].

The fatigue crack initiation behavior in ADI was investigated in [2]. It showed that, rather than at graphite nodules, primary crack initiation at the microstructural level occurred exclusively at pores, either surface or sub-surface. The number of primary initiation sites had a profound impact on the mechanism of failure and ultimately the lifetime of the specimen.

Long crack fatigue propagation, on the other hand, is the result of a complex mechanism consisting partly of the initiation and growth backwards of small cracks started at surface irregularities of the graphite nodules. Initiation of these cracks is apparently activated by the stress concentration produced when the tip of the main crack is at a sufficiently short distance from the nodule [1]. This microcrack initiation apparently depends on one or more of the following: microstructure, load ratio and stress range [2]. These small cracks eventually coalesce with the main crack front that continues to grow in the normal way until a new nodule is reached. Since several nodules can be involved in the growth process at different portions of the crack front, the average growth rate is affected by the size, shape and distribution of graphite nodules [1]. Decohesion of the interface between the graphite nodules and matrix is likely to be caused by mechanical property mismatch occurring in the stress field ahead of the advancing crack, leading to the subsequent initiation of microcracks [2].

In the near-threshold fatigue crack growth regime, the probability of occurrence of those conditions necessary for the initiation of cracks starting from nearby nodules is reduced [1]. Microstructural features such as the boundaries between prior austenite grains in the so-called “ausferrite” (bainite) microstructure were observed to significantly retard (by blocking planar slip along the austenite {111} plane) the propagation of a short fatigue crack, owing to the additional requirement to tilt and twist the crack plane for crystallographic propagation into the next grain [3, 4].

The cost increase of alloying elements used in the low-strength ADI grades has recently motivated the development of other heat treated NCI such as so-called Isothermal Ductile Iron (IDI), which is an intermediate grade between the low-strength ADI and pearlitic NCI. Since IDI is a rather new material compared to ADI, the mechanisms of fatigue crack initiation and propagation are not yet fully described and understood.

The aim of this paper is to present the IDI material and the characterization of its fatigue crack growth behavior. Near-threshold fatigue crack growth experiments performed on comparable grades of IDI and ADI 1050 will initially be reported. To investigate IDI vs. ADI as far as microstructure- ΔK_{th} property relation, the fatigue crack paths through the microstructure will be examined to identify the active growth micro-mechanisms and compared.

MATERIALS AND EXPERIMENTAL DETAILS

Material characterization

The Italian company Zanardi Fonderie established producer of NCI and ADI castings, supplied both IDI and ADI 1050 in the form of cast blocks after thermal treatment. The chemical composition of the materials and the thermal treatment conditions were according to Zanardi Fonderie internal standards. While ADI is rather known, it is stressed here that IDI combines strength comparable to pearlitic NCI grades with superior toughness properties as a result of the isothermal heat treatment, performed after casting of a special preconditioning of the metal bath. The heat

treatment basically consists of heating the NCI casting above the critical temperature followed by cooling at a rate that promotes the pearlite formation. Since alloying elements are not required for IDI production, not only the production cost is reduced, but also segregation and wall-thickness sensitivity are reduced. The resulting IDI microstructure predominantly consists of graphite nodules and ferrite/pearlite matrix with different distribution compared to the as-cast NCI. The IDI matrix is denominated “Perferritic” [5].

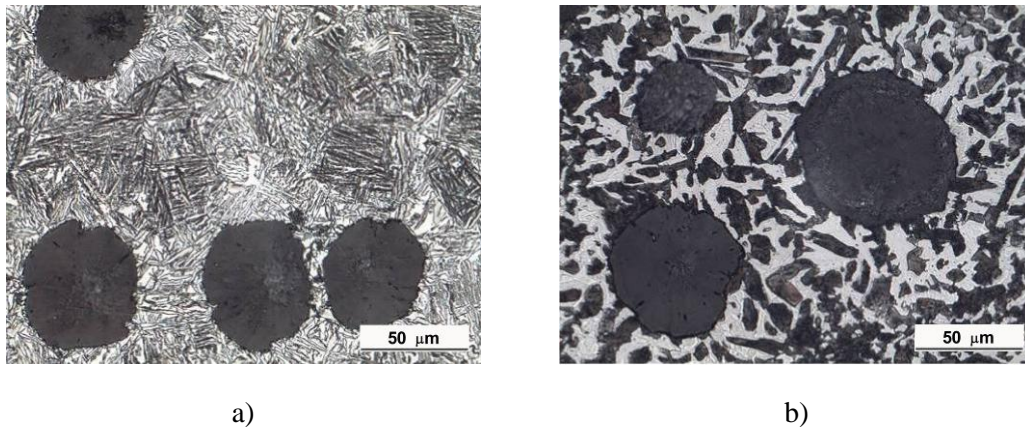


Figure 1. Characteristic microstructure of a) ADI 1050 and b) perferritic IDI, etched 3% Nital

Three CT specimens (thickness $B = 10$ mm, width $W = 50$ mm) for fatigue crack growth experiments were machined from ADI and IDI blocks, respectively. The metallographic analysis of ADI and IDI specimens was performed on light optical microscope NEOPHOT 32.

The microstructure of ADI 1050, see Fig. 1a, consists of coarse needle-shaped acicular ferrite (bainitic ferrite) in carbon-enriched retained austenite and nodular graphite no uniformly dispersed in the matrix. The IDI microstructure is a mixture of proeutectoid ferrite and pearlite, see Fig. 1b. The microstructure of IDI specimens showed higher concentration of perlite on the eutectic cells boundaries than in their central part. The volume fraction of ferrite for specimen IDI 1 was 29 %, for IDI 2 it was 27 % and for IDI 3 it was 34 %.

The graphite nodule count was almost the same, i.e. around 50 nodules per mm^2 , for the three CT specimens of ADI. It is quite low for a nodular cast iron for which the suggested number is around 200 nodules per mm^2 , [7]. The graphite fraction in the structure volume was also similar for all the specimens. In the case of IDI the nodule count was similar to ADI, i.e. around 80 nodules per mm^2 and similar for all the CT specimens.

Graphite nodule globularity, which could have influence on the fatigue crack initiation according to the stresses on the irregular shaped graphite particles edges, showed specimen-to-specimen difference. In the case of the specimen ADI 1 only 30 %

of particles had globularity higher than 80 %, for the specimen 2 it was 40 % and for the specimen 3 50 % of the graphite particles with globularity higher than 80 % was observed. Differences in graphite nodule globularity was found in the case of IDI specimens too: in specimens IDI 1 and IDI 3 only 30 % of particles had globularity higher than 80 % and the specimen IDI 2, the graphite particles globularity higher than 80 % was observed for 50 % of graphite particles.

Material testing

Fatigue crack propagation experiments were performed according to the ASTM standard E 647-08, [8], in the electromagnetic resonant testing machine Roell Amsler HFP 5100 at initial cyclic frequency of 100 Hz. A sinusoidal waveform with the constant load ratio $R = 0.1$ was applied. Preliminarily, three CT specimens of each material were precracked at a chevron starter notch. To provide sufficient visibility of fatigue crack propagation, lateral specimen surfaces were polished by 1- μm -grain-size diamond paste. CCD cameras were used to monitor the propagating cracks, while the current crack length (a) was measured by digital micrometers and recorded simultaneously with number of cycles (N). The fatigue crack propagation curves da/dN vs. K_a where $K_a = (K_{\max} - K_{\min})/2$ were thus determined [8].

The threshold stress intensity factor amplitude K_{ath} was determined using the load shedding technique [8]. This procedure involves slowly reducing the stress intensity amplitude by reducing stepwise the applied load after the crack had grown by at least 1 mm in length at the previous K_a level, and recording the crack growth rate da/dN . The crack growth threshold values K_{ath} were then identified as the values of K_a at which the crack growth rate was of the order of 10^{-10} m/cycle.

After fatigue crack propagation test, the CT specimens were broken under tensile load. Tensile properties of experimental material were measured on flat tensile testing specimens, extracted from the halves of CT specimens. Three identical tensile specimens were prepared from each CT half. A 25 kN MTS 810 testing machine equipped with extensometer model 632.31F-24 was used to perform tensile tests with displacement velocity of 0.01 mm/s.

Fatigue crack surface was examined in the SEM while the fracture profiles were investigated in the optical microscope after etching.

RESULTS AND DISCUSSION

Fatigue crack growth rates and threshold behavior

Fig. 2 shows that the fatigue crack growth data of ADI 1050 experimentally determined on three specimens fall on a single crack growth curve with a threshold valued $K_{\text{ath}} = 4 \text{ MPa}\cdot\text{m}^{1/2}$. On the contrary, three different fatigue crack growth curves were determined for the three IDI specimens. Large differences can be seen especially in the threshold values of the stress intensity factor amplitude, K_{ath} from $6 \text{ MPa}\cdot\text{m}^{1/2}$ to $10 \text{ MPa}\cdot\text{m}^{1/2}$. These values are also rather large compared to literature for NCI. Possible contribution of microstructure and of crack-microstructure interaction on the

substantially different behavior was therefore investigated and is discussed in the next section.

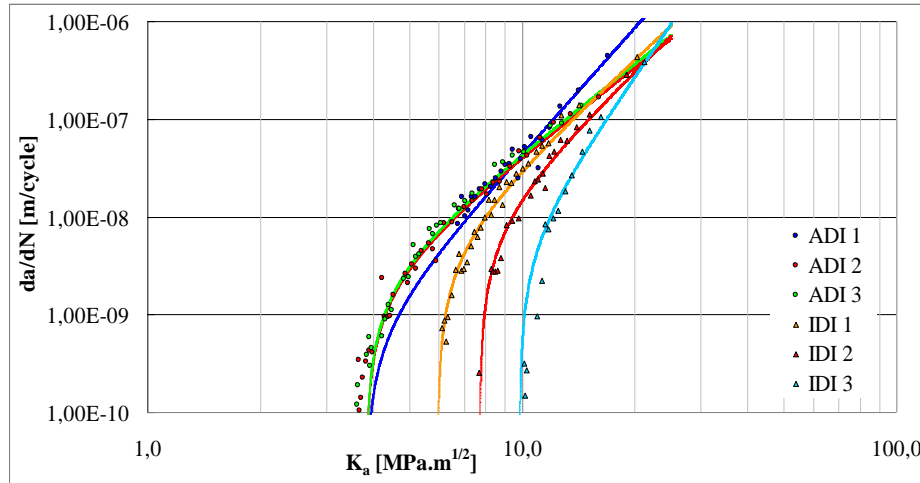


Figure 2. Fatigue crack propagation in ADI and IDI

Fatigue crack paths

The crack paths were investigated and special attention placed at two crack lengths: i) that corresponding to near-threshold condition K_{ath} (i.e. $da/dN = 10^{-9}$ m/cycles) and ii) that where $K_a = 10 \text{ MPa.m}^{1/2}$ loading condition was reached. Differences in crack patch roughness may explain such fatigue crack growth behavior. Crack tilting due to its interaction with the microstructure reduces the driving force and the resulting fracture roughness activates closure mechanisms that also reduce the driving force.

Fig. 3 shows the fracture profiles typical for all specimens of ADI and of IDI for near-threshold growth rate. The profile is macroscopically rather planar in both materials; only when the crack paths locally interacts with graphite nodules deep dimples with or without graphite nodules can be seen, Figs. 3a, b.

At the microstructural level, Fig. 3c shows transcrystalline crack propagation in ADI. Because of the typical austempered structure characterized by the presence of bainitic ferrite clusters, the crack propagated between bainitic ferrite needles oriented parallel to the fracture profile or through clusters of bainitic ferrite needles, having specific orientation. The crack paths, adjacent to the graphite nodules, follow the phase interface between graphite nodules and matrix, Fig. 3c. Locally, when graphite nodules are irregular with low globularity, the crack propagates through graphite particles. In the case of IDI specimens the fatigue crack growth corresponding to the rate of 10^{-9} m/cycles was characterized by transcrystalline propagation through the ferrite and pearlite grains. Therefore, the difference in microstructure (i.e. bainite vs. pearlite/ferrite) rather than the crack roughness may explain the higher threshold of K_a of IDI compared to ADI.

When the crack paths at the crack length of $K_a = 10 \text{ MPa.m}^{1/2}$ depth is examined the following differences are found. The fatigue fracture profile of ADI 2, Fig. 4a, shows

higher roughness compared to the condition $da/dN = 10^{-9}$ m/cycles, Fig. 3a although crack interaction with bainitic needles the crack growth direction. When the crack reaches a boundary of a needle cluster, it reorients itself in accordance to the direction of the next cluster. On the other hand, secondary cracks were observed on the fracture profile.

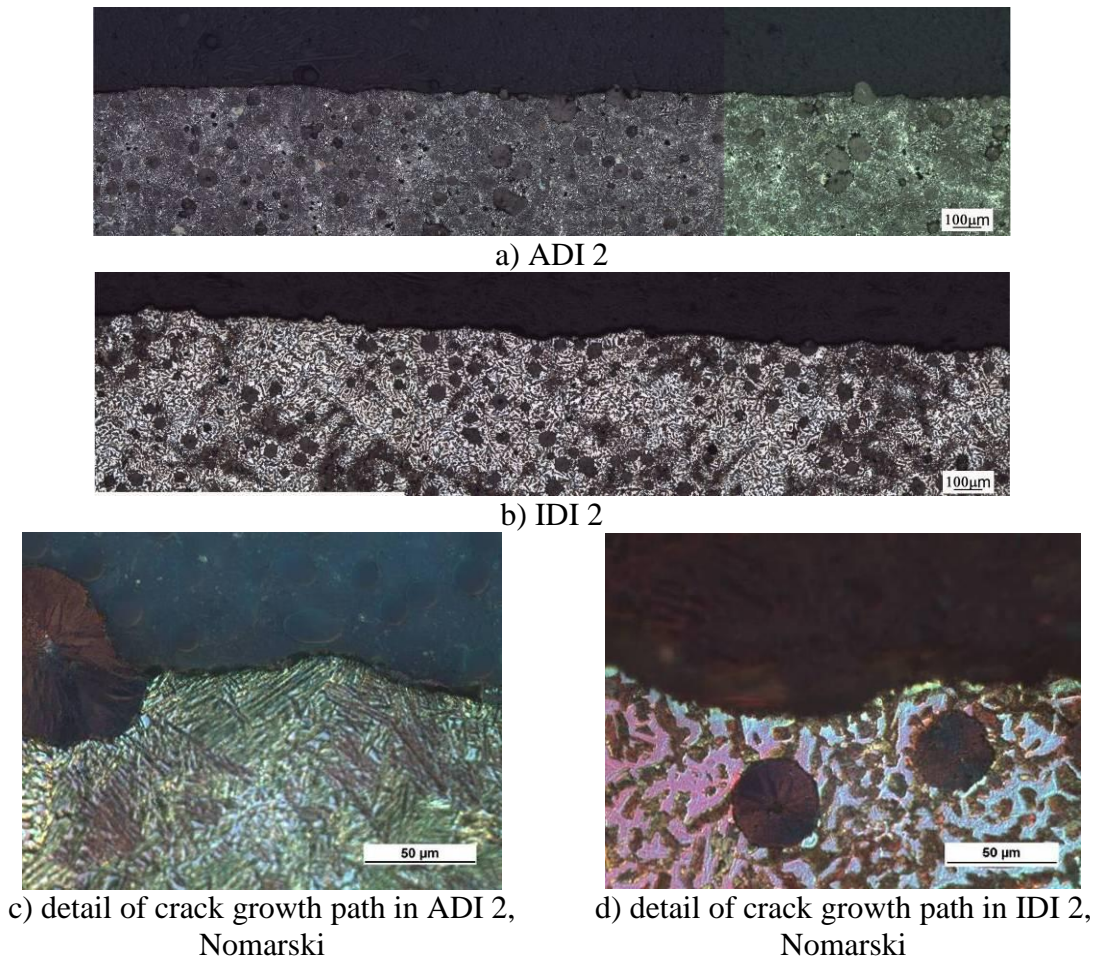


Figure 3. Fatigue fracture profile at $da/dN = 10^{-9}$ m/cycles, direction of crack propagation is from the right side, etched 3% Nital

The fatigue fracture profiles of individual IDI specimens are different and are influenced by the presence of eutectic cells (EC), Fig. 4 b, c, d, according to [9,10]. Therefore the fatigue crack propagates through a heterogeneous matrix with local ferrite/pearlite distribution difference. The mechanism of crack propagation depends on the position of the crack whether the pearlite-rich boundary where crack growth is easier or the ferrite-rich center where crack growth rate is affected by ferrite plasticity. In addition, in all the cases numerous secondary cracks are found.

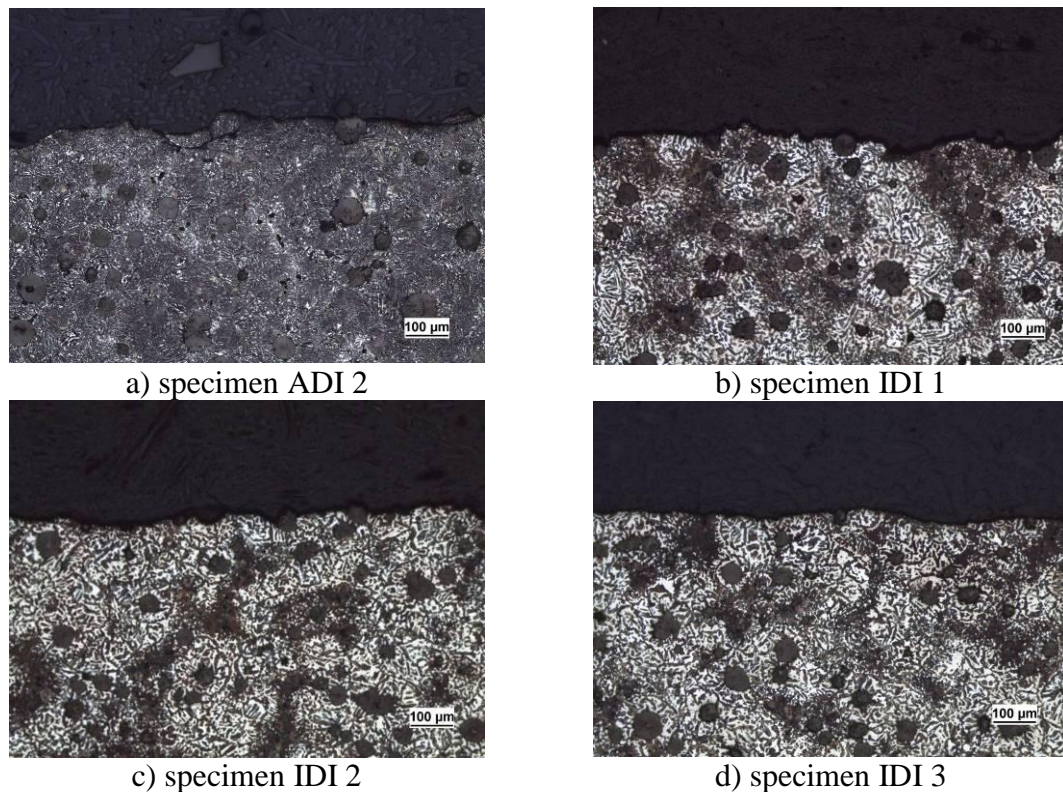


Figure 4. Fatigue fracture profile, $K_a = 10 \text{ MPa.m}^{1/2}$, direction of crack propagation is from the right side, etched 3% Nital

The previous observations of microstructure and fatigue crack paths cannot satisfactorily explain the specimen-to-specimen difference in ΔK_{th} . Therefore two other types of tests were performed on IDI: i) fracture surface roughness measurements by AFM; ii) local tensile tests.

The concept of a link between surface roughness and threshold value is often adopted to explain load ratio and material strength effects. Here the micro-roughness of the fatigue fracture surface of IDI CT specimens was measured using AFM (Atomic force microscopy). A typical 3D roughness map is shown in Fig. 5. The area investigated is about $2 \times 2 \text{ mm}^2$. The average roughness R_a was numerically extracted from the maps taken at locations associated respectively to K_{ath} and $K_a = 10 \text{ MPa.m}^{1/2}$. For IDI 1 $R_a = 8.1$ and 15.4 respectively, while for IDI 3 $R_a = 9.4$ and 12.2 respectively. The micro roughness is coherent with K_{ath} values and with the crack growth rates at $K_a = 10 \text{ MPa.m}^{1/2}$.

Three tensile specimens were also extracted from the CT specimen halves and tested in a servo hydraulic machine. The stress-strain curves are presented in Fig. 6. They show that the roughness increase of IDI a significant (i.e. roughly up to 20 %) specimen-to-specimen difference in terms of yield stress and ultimate strength. The scatter in elongation to rupture is even more significant. It appears that the microstructure is heterogeneous.

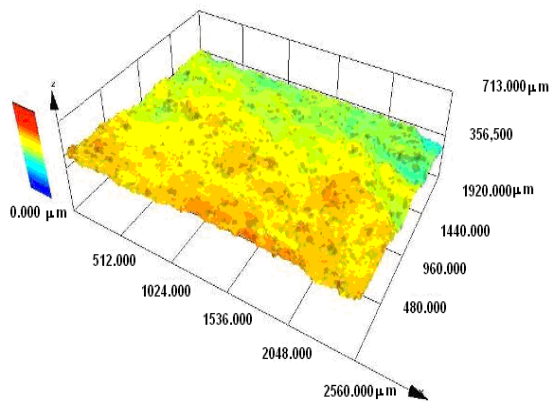


Figure 5. Typical micro roughness map of the fracture surface obtained by AFM

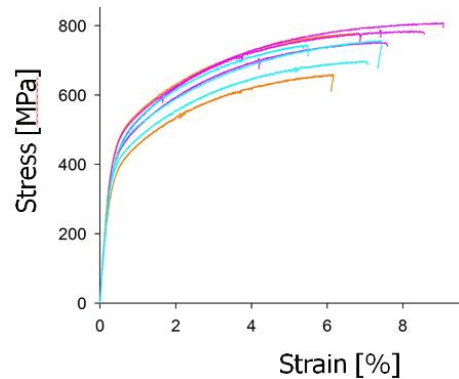


Figure 6. Stress-strain curves of IDI extracted from the three CT specimens

CONCLUSIONS

The experiments performed on comparable grades of ADI 1050 and IDI, which is a heat-treated nodular cast iron, have led to the following conclusions:

- IDI has higher K_{ath} than ADI 1050.
- The different microstructures of ADI and IDI affect the crack propagation mechanisms and crack tip direction.
- Fatigue fracture roughness is low at K_{ath} in both materials because the microstructure is very fine. The roughness increase with applied K_a and is higher in IDI than ADI because of the softer phase of the former.
- The heterogeneity of the original IDI cast bloc influenced the fatigue crack growth tests.

REFERENCES

1. Greno, G.L., Otegui, J.L., Boeri, R.E. (1999) *Int. J. Fat.* **21**, 35-43.
2. Strokes, B., Gao, N., Reed, P.A.S. (2007) *Mat. Sci. Eng. A* **445-446**, 374-385.
3. Marrow, T.J., Buffiere, J.Y., Withers, P.J., Johnson, G., Engelberg, D. (2004) *Int. J. Fat.* **26**, 717-725.
4. Marrow, T.J., Cetinel, H. (2000) *Fatigue Fract. Eng. Mater. Struct.* **23**, 425-434
5. Massagia, S. (2010) *Proc. Eng.* **2**, 1459-1476.
6. Yang, J., Putatunda, S.K. (2005) *Mat. Sci. Eng. A* **393**, 254-268.
7. Karsay, S.I. (1996) *Nodular cast iron I. Production*. Fompex. Trenčín. (in Slovak)
8. ASTM Standard E 647-08: Standard Test Method of Measurement of Fatigue Crack Growth Rates, 2009.
9. Rivera, G.L., Boeri, R.E., Sikora, J.A. (2003) *Trans. Am. Foundry Soc.* **111**, 979-989.
10. Rivera, G.L., Boeri, R.E., Sikora, J.A. (2002) *Mat. Sci. Tech.* **18**, 691-697.